An Ab Initio Investigation of the Ground and Excited Electronic State Properties of a Series of Bromine- and Iodine-Containing Singlet Carbenes

Sheryl A. Drake, Jean M. Standard, and Robert W. Quandt*

Department of Chemistry, Illinois State University, Normal, Illinois 61790-4160

Received: August 1, 2001; In Final Form: November 20, 2001

Ab initio calculations have been performed to determine the structure and energies of the ground and first excited electronic states of bromine- and iodine-containing singlet carbenes. Effective core potential basis sets augmented with polarization functions were utilized at the CASSCF, CASPT2, and CISD levels of theory. Validation of the effective core potential basis sets for the ground and excited states of the singlet carbenes was carried out by comparison with previous results from all-electron basis set calculations. As was the case in previous studies of chlorine- and fluorine-containing halocarbenes, the bromine- and iodine-containing singlet carbenes are characterized by small bond angles in their ground states, ranging from 100° to 112°, and dramatically larger bond angles in their first excited states, ranging from 125° to 132°. This increase is due to the promotion of an electron from a carbon lone pair orbital coplanar with the carbon−halogen bonds to a carbon p-type orbital perpendicular to the bonds. Adiabatic transition energies for transitions from the ground to first excited state for the singlet carbenes determined at the CASPT2(18,12) and CISD levels range from 21 277 to 10 870 cm^{-1} and are in excellent agreement with experimental measurements where comparisons are available.

I. Introduction

It has been shown conclusively that the use of chlorofluorocarbons (CFCs) and halons as refrigerants, aerosol propellants, and etchants in semiconductor manufacturing has significantly contributed to stratospheric ozone destruction. The enactment of the Montreal Protocols in 1987, along with the 1990 London revisions, called for the total phaseout of these compounds by 1996.[1] Since 1987, the search for suitable alternatives to CFCs and halons has centered on hydrochlorofluorocarbons (HCFCs) and hydrofluorocarbons (HFCs). These compounds' environmental acceptability stems from the fact that the presence of one or more C−H bonds allows them to be oxidized relatively quickly by OH radicals in the troposphere. This gives HCFCs and HFCs a mean atmospheric lifetime on the order of 3−6 months as opposed to the decade-long lifetimes associated with CFCs. However, because of various atmospheric mixing phenomena, some of these HCFCs can reach the upper atmosphere. For example, measurements taken during the ATLAS-3 mission in 1994 showed dramatic increases in the amount of HCFC-22 in the stratosphere. Of course, once in the stratosphere, these species are exposed to very short wavelength (>200 nm) light, which may result in photodissociation.

One set of possible photoproducts from the breakdown of both HCFCs and halons are halocarbenes. In addition to their importance in atmospheric chemistry, halocarbenes are also of interest because of their role as intermediates in organic synthesis and in gas-phase combustion.[2,3] This has led to numerous theoretical studies of smaller carbenes such as CH_2, CF_2, CCl_2, and HCF. However, because of the different reactivities of the singlet and triplet states, a majority of these works have concentrated on either the structure of the triplet state or the singlet−triplet energy gap.[4−13]

Experimental studies performed on halocarbenes have also been limited to the smaller XCY species (where X and Y = H, Cl, or Br).[14−25] In these gas-phase studies, the ground electronic states were found to have singlet multiplicity (the triplet ground state of CH_2 being the notable exception) with A_1 orbital symmetry for the C_{2v} molecules and A′ for the C_s molecules. The first singlet excited state above the ground state has B_1 (C_{2v}) or A″ (C_s) orbital symmetry in agreement with theory. For reasons to be discussed shortly, emission from the first singlet excited states of these carbenes tends to be too weak for fluorescence dispersal studies.

Only a few groups have conducted ab initio investigations of the singlet excited states of halocarbenes. As was the case with the experimental work mentioned above, most of these studies have been limited to the smaller halocarbenes.[26−32] With the use of the CASSCF, CASPT2, and MRCI methods, it was found that, in general, upon excitation from the ground to first excited singlet state, the C−X and C−Y bond lengths change very little, while the X−C−Y bond angle opens up from about 100°−110° to around 120°−130°. It should be also noted that, for all of the halocarbenes except CF_2, the inversion barrier from a bent to linear structure is predicted to be less than the dissociation energy at the CASPT2 level of theory.[27] This leads to Renner−Teller coupling between the excited and ground states, which greatly enhances the odds of a nonradiative transition back to the ground state. This effect also explains the weak emission seen by Clouthier and others,[16,17] as well as the lack of experimental observation of halocarbenes such as CBrI and CI_2.

While a few theoretical and experimental studies have focused on the singlet electronic excited states of bromine-containing carbenes, to the best of our knowledge no studies have been performed on the singlet electronic excited states of iodine-containing carbenes. This is unfortunate because the large spin−orbit couplings of the heavier halogens create unique electronic properties. This lack of data is most likely because the large masses of the bromine and iodine atoms make them difficult to

10.1021/jp012967a CCC: $22.00
Published on Web 01/22/2002

observe experimentally (due to Renner−Teller coupling) and their large numbers of electrons make them computationally costly. The experimental problem of Renner−Teller coupling can be overcome by using an absorption technique such as cavity ringdown laser absorption spectroscopy (CRDLAS). However, to use this technique to observe these halocarbenes experimentally, their excitation wavelengths must first be known. As stated above, there is currently a lack of information on the excited states of the heavier halocarbenes. To obtain reasonable estimates of absorption wavelengths and to address the lack of theoretical data on bromine- and iodine-containing halocarbenes, we report the ground and excited-state structures and energies for a series of these species, as well as adiabatic transition energies, using the CASSCF, CASPT2, and CISD levels of theory. Because of the large numbers of electrons in the bromine- and iodine-containing halocarbenes, the calculations will be performed using effective core potentials (ECPs) to represent the core electrons and double-ζ plus polarization quality basis sets to represent the valence electrons. It is important, therefore, to assess the validity of the use of ECP basis sets for both the ground and excited states of the singlet bromo- and iodocarbenes studied in this work. Where available, the results obtained in this work will be compared with all-electron basis set calculations.

II. Methods

Ground and first excited electronic states of bromine- and iodine-containing singlet halocarbenes were studied using a variety of ab initio methods. All of the calculations employed the Stevens, Basch, Krauss, Jasien, and Cundari (SBKJC) effective core potential along with the corresponding valence-only basis set of double-ζ quality.[33−35] The basis set was augmented by adding three sets of d-type polarization functions to non-hydrogen atoms and three sets of p-type polarization functions to hydrogen atoms. For HCX (X = Cl, Br, or I) singlet halocarbenes, 63 functions comprise the basis set, while for XCY (X and Y = F, Cl, Br, or I) singlet halocarbenes, the basis set consists of 78 functions.

The PC GAMESS[36] version of the GAMESS (U. S.) electronic structure package[37] was utilized on a Windows-based personal computer for CISD calculations of ground and excited electronic states to obtain optimized geometries, electronic energies, and adiabatic transition energies. Full singles and doubles CI calculations were carried out for the 12 valence electrons of HCX halocarbenes and for the 18 valence electrons of XCY halocarbenes. Convergence criteria for the geometry optimizations were that the RMS gradient was less than or equal to 3×10^{-5} and the maximum component of the gradient was less than or equal to 1×10^{-4}.

For the CASSCF and CASPT2 calculations, the software package MOLPRO[38] running on a Silicon Graphics/Cray Origin2000 at the National Center for Supercomputing Applications in Urbana, IL, was employed. Full geometry optimizations were carried out for the ground and first excited electronic states of the singlet halocarbenes. For the CASSCF and CASPT2 geometry optimizations, the convergence criteria were 3×10^{-4} for the rms gradient and 5×10^{-4} for the maximum component of the gradient.

Two different levels of CASSCF and CASPT2 calculations were completed. The first series of calculations involved using two electrons in two active orbitals. The two electrons included in the calculations are those that correspond to the lone pair of electrons on the carbon atom. The two active orbitals employed are the lone pair orbital and the empty p-type orbital on the carbon atom. The two electron, two orbital CASSCF and CASPT2 calculations provide a minimal representation of the singlet halocarbene systems; however, to determine more accurate adiabatic transition energies, a full valence active space was utilized in a second series of calculations. CASSCF and CASPT2 calculations for the HCX halocarbenes were carried out using 12 valence electrons and 9 active orbitals. For the XCY halocarbenes, the calculations included 18 valence electrons and 12 active orbitals.

TABLE 1: Results for Ground Electronic States of XCBr and XCI Singlet Carbenes

	CISD	CASSCF-(2,2)	CASPT2-(2,2)	CASSCF-(18,12)[a]	CASPT2-(18,12)[a]
			HCBr		
r(H−C), Å	1.120	1.099	1.110	1.099	1.109
r(C−Br), Å	1.876	1.889	1.875	1.897	1.894
θ(H−C−Br), deg	100.64	101.72	100.68	101.16	99.91
			FCBr		
r(F−C), Å	1.289	1.274	1.303	1.284	1.315
r(C−Br), Å	1.932	1.939	1.942	2.001	1.982
θ(F−C−Br), deg	106.57	106.81	106.86	106.51	106.45
			ClCBr		
r(Cl−C), Å	1.710	1.710	1.717	1.746	1.738
r(C−Br), Å	1.902	1.901	1.912	1.951	1.940
θ(Cl−C−Br), deg	109.74	110.12	109.70	109.58	109.25
			CBr_2		
r(C−Br), Å	1.893	1.891	1.900	1.939	1.930
θ(Br−C−Br), deg	110.11	110.49	110.09	109.83	109.61
			ICBr		
r(I−C), Å	2.114	2.116	2.120	2.174	2.157
r(C−Br), Å	1.886	1.883	1.893	1.931	1.924
θ(I−C−Br), deg	111.12	111.42	111.04	110.72	110.56
			HCI		
r(H−C), Å	1.121	1.099	1.112	1.132	1.121
r(C−I), Å	2.080	2.101	2.075	2.123	2.103
θ(H−C−I), deg	100.40	101.37	100.35	99.70	99.33
			FCI		
r(F−C), Å	1.287	1.266	1.298	1.281	1.313
r(C−I), Å	2.171	2.173	2.174	2.261	2.217
θ(F−C−I), deg	107.30	107.28	107.47	107.19	107.57
			ClCI		
r(Cl−C), Å	1.705	1.712	1.707	1.740	1.734
r(C−I), Å	2.125	2.134	2.129	2.190	2.170
θ(Cl−C−I), deg	110.76	110.69	110.87	110.49	110.25
			CI_2		
r(C−I), Å	2.104	2.106	2.109	2.162	2.149
θ(I−C−I), deg	112.29	112.49	112.12	111.55	111.64

[a] For HCBr and HCI, the higher level calculations were performed using 12 electrons in 9 active orbitals.

III. Results and Discussion

A. Ground-State Calculations. The ground-state ($^1A_1$ or $^1A'$) structures and energies of a series of bromo- and iodocarbenes are reported in Table 1. Note that the molecules HCBr, FCBr, and CBr_2 were included to determine the effectiveness of the ECP double-ζ plus polarization basis sets used in this work relative to the all-electron triple-ζ plus polarization sets used in previous works.[27,30,32]

The general structure of all species is bent, with small H−C−X or X−C−Y bond angles, similar in magnitude to the bond angle of CH_2. These bond angles varied from about 100° for the small species, such as HCBr and HCI, to around 110° for the larger species such as CBr_2 and CI_2. While having a bent ground-state structure for a stable 18 valence electron molecule is not surprising, the extent to which the molecule is bent is rather surprising. For example, the ground states of O_3

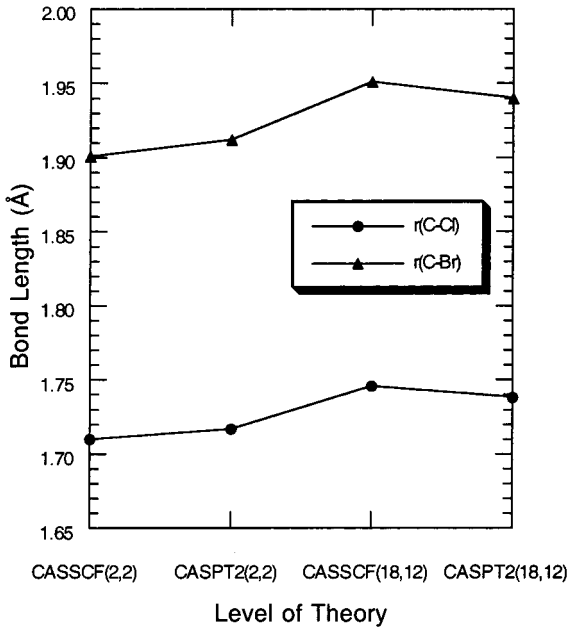

Figure 1. Trends in C−Cl and C−Br bond lengths for the ground singlet electronic state of ClCBr computed at the CASSCF and CASPT2 levels of theory.

and SO_2 have bond angles of 116° and 119°, respectively,[39] while the much larger CI_2 has a calculated angle of only 111°. The relatively tight bond angle of the ground states is easily explained by a Walsh orbital overlap diagram. The doubly occupied $^1A_1$ ($^1A'$) bent ground state has significantly more orbital overlap between the carbon−halogen s and p orbitals than does the linear $^1\pi_u$ state. Therefore, any occupation of the $^1A_1$ ($^1A'$) orbital lowers the energy of the bent molecular structure relative to the linear structure. The increased bond angle of the larger species is simply due to steric repulsion between the large halogen substituents. All of the bond lengths shown in Table 1 are typical for carbon−hydrogen or carbon−halogen single bonds.

In comparing the geometries obtained from the CASSCF and CASPT2 methods for the ground electronic states of the singlet halocarbenes, some trends are observed. First, little variation in carbon−hydrogen bond lengths is noted, with variations for HCBr and HCI C−H bond lengths of less than 0.02 Å. Second, bond angles for all of the carbenes are relatively insensitive to the level of theory, with variations for each molecule of less than 1.3°.

Trends in carbon−halogen bond lengths calculated using the CASSCF and CASPT2 methods are illustrated using the example of ClCBr, shown in Figure 1. The carbon−halogen bonds generally lengthen at the CASPT2(2,2) level compared to the CASSCF(2,2) level. The exceptions are the carbon−halogen bonds in the HCX carbenes, which show small decreases of 0.01−0.03 Å. The increases in carbon−halogen bond lengths in XCY carbenes are modest, with none being larger than 0.03 Å. On the other hand, when comparing CASSCF(18,12) to CASPT2(18,12) results, a decrease in carbon−halogen bond lengths at the CASPT2 level is observed for most of the carbenes, with variations ranging from 0.01 to 0.04 Å.

The most significant trend, as illustrated in Figure 1, is the lengthening of carbon−halogen bonds at both the CASSCF and CASPT2 levels when the active space is increased from (2,2) to (18,12) for XCY carbenes or (12,9) for HCX carbenes. Many of the increases in bond lengths are substantial, particularly at the CASSCF level. For example, many of the CASSCF(18,12) or (12,9) bond lengths are 0.02−0.06 Å longer than the corresponding CASSCF(2,2) values. The largest increase is seen for the C−I bond of FCI, which lengthens by 0.09 Å at the CASSCF(18,12) level. Increases in bond lengths are more modest at the CASPT2(18,12) or (12,9) level compared to those at the CASPT2(2,2) level, though many are still around 0.03−0.04 Å longer.

TABLE 2: Comparison of Theory and Experiment for Ground State ($^1A_1$ or $^1A'$) Carbenes

	CISD[a]	CASPT2(18,12)[a,b]	previous theoretical	experiment
		HCBr		
r(H−C), Å	1.120	1.109	1.097, 1.101[c]	1.110[d]
r(C−Br), Å	1.876	1.894	1.861, 1.847[c]	1.857[d]
θ(H−C−Br), deg	100.64	99.91	101.9, 101.2[c]	101.00[d]
		FCBr		
r(F−C), Å	1.289	1.315	1.287[e]	
r(C−Br), Å	1.932	1.982	1.898[e]	
θ(F−C−Br), deg	106.57	106.45	107.2[e]	
		CBr_2		
r(C−Br), Å	1.893	1.930	1.882[e]	1.865[f]
θ(Br−C−Br), deg	110.11	109.61	110.0[e]	110.7[f]

[a] This work. [b] For HCBr, the higher level calculations were performed using 12 electrons in 9 active orbitals. [c] Li and Francisco.[32] Values reported are for the TZ2P and 6-311++G(3df,pd) basis sets, respectively, at the CISD level of theory. [d] Sears and co-workers.[24] [e] Bacskay, Kable, and co-workers.[27,30] Values reported are for the cc-pVTZ basis set at the CASPT2(18,12) level of theory. [f] Xu and Harmony.[15]

As mentioned previously, there have been many studies, both experimental and computational, on the ground-state halocarbenes. However, only a few of these have focused on both the ground and excited singlet states together, which is necessary for determination of excitation energies. For the ground state, the only species for which both previous theoretical and experimental results are available for comparison are HCBr, FCBr, and CBr_2.[27,30,32] These previous results along with the CISD and CASPT2(18,12) values from this work are shown together in Table 2. The results for HCBr shown in Table 2 agree well with previous computational studies. Li and Francisco[32] studied the singlet ground state of HCBr using the TZ2P and 6-311++G(3df,pd) basis sets at the MP2, CISD, and CCSD(T) levels of theory. Of particular interest is their use of the CISD method, which yielded C−H bond lengths of 1.097 Å (TZ2P) and 1.101 Å (6-311++G(3df,pd)), which were about 0.02 Å lower than the CISD value in Table 2. The CISD C−Br bond length of 1.876 Å calculated in this work was only slightly larger (0.015 Å) than Li and Francisco's TZ2P CISD value of 1.861 Å. The basis set difference is somewhat more pronounced for the 6-311++G(3df,pd) CISD computations, with Li and Francisco's bond length of 1.847 Å being 0.029 Å shorter than the C−Br bond length computed in this work. The HCBr bond angles in both works agree quite well; they are within 0.8° of each other. These comparisons suggest that the SBKJC effective core potential double-ζ basis set augmented with polarization functions performs well when compared with all-electron basis triple-ζ plus polarization sets.

The CBr_2 and FCBr geometrical parameters calculated in this work agree well with those of Bacskay, Kable, and co-workers.[27,30] For CBr_2, C−Br bond lengths of 1.926 and 1.882 Å and bond angles of 110.3° and 110.0° were obtained in the previous studies at CASSCF(18,12) and CASPT2(18,12) levels,

respectively. Calculations at the same level of theory from this work in Table 2 yielded values of 1.939 and 1.930 Å for the bond lengths and 109.83° and 109.61° for the bond angles. The longer bond lengths of the present results lead to somewhat smaller bond angles than those determined in the previous literature studies. The minor differences in bond lengths and bond angles are most likely due to the different basis sets used, because Bacskay, Kable, and co-workers used the all-electron correlation-consistent polarized valence triple-ζ (cc-pVTZ) basis for their study. This basis set includes f-type polarization functions, the inclusion of which leads to a shortening of the carbon−halogen bonds. For example, addition of one set of f-type polarization functions to the basis set used in this work leads to a contraction of the C−Br bond of CBr_2 by 0.02 Å for both the ground and excited electronic states at the CASPT2-(18,12) level. A similar effect is observed for the C−I bond of CI_2. Any additional discrepancies between the current work and literature are likely due to the use of the ECP double-ζ quality basis as opposed to the triple-ζ basis used in the literature studies.

Similarly for FCBr, Bacskay, Kable, and co-workers obtained C−F bond lengths of 1.278 and 1.287 Å, C−Br bond lengths of 1.948 and 1.898 Å, and bond angles of 106.9° and 107.2° at the CASSCF(18,12) and CASPT2 levels, respectively. The same calculations from this work in Table 2 yielded values of 1.284 and 1.315 Å for the C−F bond lengths and 2.001 and 1.982 Å for the C−Br bond lengths, along with 106.51° and 106.45° for bond angles, respectively, at the CASSCF(18,12) and CASPT2(18,12) levels. Once again, the differences are likely due to the different basis sets used in each study. Small relativistic effects for the Br atom may also contribute to the differences observed between the present results and literature. However, for molecules containing third-row elements, relativistic effects are generally small. For example, calculations on molecules containing Se showed relativistic effects on the bond lengths of less than 0.003 Å and little or no effect on bond angles.[40] On the other hand, relativistic effects are expected to be more significant for molecules containing iodine; thus, the use of the SBKJC relativistic effective core potential is essential for the accurate description of iodocarbenes.

The calculated C−Br bond lengths and angles in Table 2 also agree well with the experimental values of Xu and Harmony for CBr_2[15] as well as the experimental values for HCBr from Sears and co-workers.[24] For CBr_2, the bond lengths calculated in this work are somewhat longer (0.026−0.074 Å) and the bond angles slightly smaller (0.21°−1.09°) than those obtained by Xu and Harmony. For HCBr, the C−H bond lengths are in very good agreement with Sears and co-workers at all levels of theory. In particular, the value of 1.110 Å at the CASPT2(2,2) level of theory is in perfect agreement with experiment. The largest discrepancy is only 0.011 Å for both the CASSCF(2,2) and CASSCF(18,12) levels. Similarly, the C−Br bond lengths and H−C−Br bond angles in Table 2 are in good agreement with experiment. For the bond lengths, the differences varied from 0.018 to 0.040 Å, while the differences for the bond angles ranged from 0.16° to 1.07°.

B. Excited-State Results. The excited-state geometries and energies for the various singlet halocarbenes are reported in Table 3. Some of the CASSCF and CASPT2 geometry optimizations failed to converge for the excited states of the FCBr and FCI molecules. In fact, convergence to an optimized structure was achieved only at the CASPT2(18,12) level for these molecules. This behavior was also noted by Bacskay, Kable, and co-workers in their study of FCBr.[30] The difficulty of obtaining optimized structures for FCBr and FCI is likely due to a shallow well on the excited-state potential surface. In addition, for the carbenes with C_s symmetry, the CISD calculations failed to converge. As a result, work is in progress to determine optimized structures for the excited states of these singlet carbenes using the multireference configuration interaction (MRCI) method, which has been shown to be successful in the case of CFBr.[30]

TABLE 3: Results for First Excited Electronic States of XCBr and XCI Singlet Carbenes

	CISD	CASSCF-(2,2)	CASPT2-(2,2)	CASSCF-(18,12)[a]	CASPT2-(18,12)[a]
			HCBr		
r(H−C), Å	1.100	1.077	1.089	1.080	1.090
r(C−Br), Å	1.814	1.815	1.790	1.832	1.812
θ(H−C−Br), deg	128.02	132.95	130.91	129.43	129.49
			FCBr		
r(F−C), Å	DNC[b]	DNC[b]	DNC[b]	DNC[b]	1.320
r(C−Br), Å					1.930
θ(F−C−Br), deg					124.81
			ClCBr		
r(Cl−C), Å	DNC[b]	1.662	1.655	1.705	1.675
r(C−Br), Å		1.831	1.838	1.907	1.862
θ(Cl−C−Br), deg		132.06	131.05	128.76	130.27
			CBr_2		
r(C−Br), Å	1.852	1.830	1.830	1.896	1.856
θ(Br−C−Br), deg	126.99	132.63	131.06	128.95	130.28
			ICBr		
r(I−C), Å	DNC[b]	2.033	2.033	2.126	2.064
r(C−Br), Å		1.829	1.825	1.886	1.853
θ(I−C−Br), deg		133.96	131.74	129.45	131.01
			HCI		
r(H−C), Å	1.102	1.078	1.090	1.081	1.090
r(C−I), Å	2.034	2.010	1.973	2.027	2.001
θ(H−C−I), deg	126.29	135.07	132.33	130.22	130.09
			FCI		
r(F−C), Å	DNC[b]	DNC[b]	DNC[b]	DNC[b]	1.308
r(C−I), Å					2.426
θ(F−C−I), deg					121.69
			ClCI		
r(Cl−C), Å	DNC[b]	1.663	1.654	1.702	1.676
r(C−I), Å		2.035	2.048	2.157	2.073
θ(Cl−C−I), deg		133.24	131.61	128.91	131.03
			CI_2		
r(C−I), Å	2.070	2.031	2.022	2.108	2.058
θ(I−C−I), deg	129.109	135.63	132.58	130.38	131.79

[a] For HCBr and HCI, the higher level calculations are performed using 12 electrons in 9 active orbitals. [b] DNC = Did not converge.

At all levels of theory, the $^1B_1$ ($^1A''$) state is characterized by a dramatic increase in the bond angle and a shortening of the carbon−halogen bond lengths relative to the ground-state values. This is a well-documented behavior of carbenes. The increase in bond angle of the excited state can once again be explained by using a Walsh diagram and the fact that the transition is from the $^1A_1$ ($^1A'$) to the $^1B_1$ ($^1A''$) surface. As stated previously, the $^1A_1$ ($^1A'$) molecular orbital can significantly increase overlap of its constituent atomic orbitals by decreasing the bond angle to 90°. The corresponding π_u orbital for the linear molecule contains no s character and also contains a node, making it higher in energy. The excited state $^1B_1$ ($^1A''$) orbital is essentially a nonbonding p orbital on the carbon atom. This corresponds to the π_u orbital for the linear molecule as well and is essentially degenerate energetically. Because the $^1A_1$ ($^1A'$) and $^1B_1$ ($^1A''$) correspond to the same π_u state in the linear molecule, Renner−Teller coupling of the two states is possible if the inversion barrier is smaller than the dissociation energy.

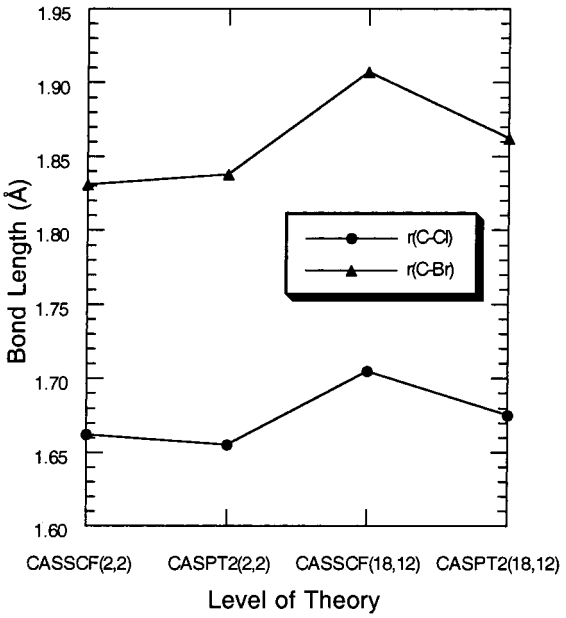

Figure 2. Trends in C−Cl and C−Br bond lengths for the first excited singlet electronic state of ClCBr computed at the CASSCF and CASPT2 levels of theory.

The decrease in carbon−halogen bond lengths occurs because, in the ground state, the lone pair electrons on the carbon atom are in an sp^2 hybridized orbital that is coplanar with both the C−X and C−Y bonds. The resulting repulsion between this lone pair and the electrons on the halogens lengthens the bonds slightly. As stated above, the excited $^1B_1$ ($^1A''$) state is a nonbonding p orbital on the carbon atom that is perpendicular to the plane formed by the carbon−halogen bonds. This removes the portion of the force vector directed along the bond axis, allowing the bonds to shorten. It also helps explain, using simple VSEPR theory, why the bond angle increases upon excitation.

A number of trends in the geometrical parameters of the excited-state halocarbenes are evident. First, calculated values of the C−H bonds for the excited-state carbenes show little variation when CASSCF and CASPT2 results are compared. Bond lengths range from 1.08 to 1.09 Å, which is about 0.02−0.03 Å shorter than the C−H bond lengths computed for the ground-state carbenes.

Next, trends in carbon−halogen bond lengths for the excited state carbenes are once again illustrated using the example of ClCBr, shown in Figure 2. Only small variations in carbon−halogen bond lengths are observed when comparing results from CASSCF(2,2) and CASPT2(2,2) levels. Bond lengths vary by 0.01−0.04 Å, with the more substantial changes occurring for the carbon−halogen bonds of HCBr and HCI. Larger deviations in the carbon−halogen bond lengths are found for the CASSCF-(18,12) results for XCY carbenes or CASSCF(12,9) results for HCX carbenes relative to the CASPT2(18,12) or (12,9) results. Carbon−halogen bonds generally decrease at the CASPT2-(18,12) or (12,9) level by 0.02−0.08 Å relative to the CASSCF-(18,12) or (12,9) values.

As was observed for the ground state carbenes, the most significant differences in the CASSCF and CASPT2 results are the fairly large increases in carbon−halogen bond lengths when the active space is increased from (2,2) to (18,12) for XCY carbenes or (12,9) for HCX carbenes. This increase is illustrated by the results shown for ClCBr in Figure 2. For example, bond lengths in XCY carbenes increase dramatically by 0.04−0.12 Å at the CASSCF(18,12) level relative to the CASSCF(2,2) level. At the CASPT2(18,12) level, the change compared to the CASPT2(2,2) level is not as dramatic, though increases of 0.01−0.04 Å in carbon−halogen bonds are observed.

TABLE 4: Comparison of Theory and Experiment for Excited State ($^1B_1$ or $^1A''$) Carbenes

	CISD[a]	CASPT2-(18,12)[a,b]	previous CASPT2-(18,12)[c]	experiment[d]
		HCBr		
r(H−C), Å	1.100	1.090		
r(C−Br), Å	1.814	1.812		
θ(H−C−Br), deg	128.02	129.49		
T_e, cm^{-1}	12 643	11 712		11 972[e]
		FCBr		
r(F−C), Å	DNC[f]	1.320	1.308	
r(C−Br), Å		1.930	1.842	
θ(F−C−Br), deg		124.81	126.5	
T_e, cm^{-1}		21 369	18 190	20 906[c]
		CBr_2		
r(C−Br), Å	1.852	1.856	1.800	1.796[g]
θ(Br−C−Br), deg	126.99	130.28	133.1	131.3[g]
T_e, cm^{-1}	15 344	15 192	14 114	15 093[g], 14 885[h]

[a] This work. [b] For HCBr, the higher level calculations were performed using 12 electrons in 9 active orbitals. [c] Bacskay, Kable, and co-workers.[27,30] [d] All experimentally measured values are T_{oo} rather than T_e. [e] Sears and co-workers.[24] [f] DNC = Did not converge. [g] Xu and Harmony.[15] Note that the bond lengths and bond angles are extrapolated from ground-state values. [h] Zhou et al.[18]

Finally, larger variations in the excited-state bond angles are observed than those found for the ground-state values when comparing the different CASSCF and CASPT2 results. For example, bond angles show rather large decreases of 3°−5° at the CASSCF(18,12) or CASSCF(12,9) levels relative to those at the CASSCF(2,2) level. Changes in bond angles are not so dramatic at the CASPT2 level, though the bond angles determined at the CASPT2(18,12) or CASPT2(12,9) level are 1°−2° smaller than those determined at the CASPT2(2,2) level.

As was the case for the ground state, the calculated bond lengths and angles of FCBr and CBr_2 from this work agree reasonably well with those of Bacskay, Kable, and co-workers[27,30] using the same levels of theory and are reported together in Table 4. For FCBr, the C−F bonds from Table 4 agree to within 0.016 Å when comparing the CASSCF(18,12) and CASPT2(18,12) results to those of Bacskay, Kable, and co-workers. At the same levels of theory, the C−Br bond length determined from our calculations is within 0.01 Å of literature results at the CASSCF(18,12) level but is 0.04 Å longer at the CASPT2(18,12) level. As discussed previously, it is likely that these variations are due to differences in the ECP double-ζ plus polarization basis sets utilized in this work and the all-electron triple-ζ plus polarization basis sets used in the literature studies.

There is much less experimental information available on the excited states of these molecules. However, using CCl_2 and CF_2 as examples, Xu and Harmony[15] argued that the bond angle of CBr_2 should increase to 131.3°, an increase of 20.6° over the ground-state value. The excited-state bond angles calculated for CBr_2 in this work vary from a low of 126.99° at the CISD level to 132.63°. Changes in the CBr_2 bond angle relative to the ground-state bond angle at different levels of theory range from 16.88° (CISD) to 22.14° (CASSCF(2,2)). These trends are in general agreement with the extrapolated predictions of Xu and Harmony. In addition, Xu and Harmony predicted a C−Br bond length of 1.796 Å, which is 0.056−0.06 Å shorter than the results of this work.

C. Adiabatic Transition Energies. The adiabatic energy differences for the $^1B_1 \leftarrow {}^1A_1$ ($^1A'' \leftarrow {}^1A'$) transitions are listed

TABLE 5: Adiabatic Transition Energies for XCBr and XCI Singlet Carbenes[a,,,]

	CISD	CASSCF(2,2)	CASPT2(2,2)	CASSCF(18,12)[b]	CASPT2(18,12)[b]
			HCBr		
Gnd St *E*, au	−19.343 640	−19.112 172	−19.347 754	−19.159 095	−19.355 390
Exc St *E*, au	−19.285 998	−19.043 370	−19.299 060	−19.093 213	−19.302 026
Adiab Δ*E*, au	0.057 641	0.068 802	0.048 694	0.065 882	0.053 363
Adiab Δ*E*, cm^{-1}	12 643	15 100	10 687	14 459	11 712
			FCBr		
Gnd St *E*, au	−42.829 021	−42.430 158	−42.866 573	−42.509 065	−42.866 669
Exc St *E*, au	DNC[c]	DNC[c]	DNC[c]	DNC[c]	−42.769 306
Adiab Δ*E*, au					0.097 363
Adiab Δ*E*, cm^{-1}					21 369
			ClCBr		
Gnd St *E*, au	−33.597 270	−33.236 819	−33.629 837	−33.302 866	−33.640 912
Exc St *E*, au	DNC[c]	−33.148 841	−33.563 399	−33.218 241	−33.567 300
Adiab Δ*E*, au		0.087 978	0.066 438	0.084 625	0.073 612
Adiab Δ*E*, cm^{-1}		19 309	14 581	18 573	16 156
			CBr_2		
Gnd St *E*, au	−32.023 995	−31.688 087	−32.055 739	−31.757 511	−32.067 549
Exc St *E*, au	−31.954 039	−31.606 018	−31.994 439	−31.678 044	−31.998 330
Adiab Δ*E*, au	0.069 956	0.082 069	0.061 300	0.079 467	0.069 219
Adiab Δ*E*, cm^{-1}	15 344	18 012	13 454	17 441	15 192
			ICBr		
Gnd St *E*, au	−30.073 568	−29.753 197	−30.105 463	−29.824 851	−30.118 391
Exc St *E*, au	DNC[c]	−29.681 635	−30.054 720	−29.754 237	−30.058 440
Adiab Δ*E*, au		0.071 562	0.050 743	0.070 614	0.059 951
Adiab Δ*E*, cm^{-1}		15 706	11 137	15 498	13 158
			HCI		
Gnd St *E*, au	−17.394 008	−17.178 391	−17.397 815	−17.232 856	−17.409 579
Exc St *E*, au	−17.341 666	−17.116 472	−17.356 239	−17.165 918	−17.360 113
Adiab Δ*E*, au	0.052 342	0.061 920	0.041 576	0.066 938	0.049 466
Adiab Δ*E*, cm^{-1}	11 481	13 590	9 125	14 691	10 856
			FCI		
Gnd St *E*, au	−40.469 880	−40.474 291	−40.906 156	−40.574 330	−40.915 530
Exc St *E*, au	DNC[c]	DNC[c]	DNC[c]	DNC[c]	−40.835 759
Adiab Δ*E*, au					0.079 771
Adiab Δ*E*, cm^{-1}					17 508
			ClCI		
Gnd St *E*, au	−31.646 371	−31.301 688	−31.678 914	−31.369 894	−31.691 244
Exc St *E*, au	DNC[c]	−31.225 268	−31.624 491	−31.295 786	−31.628 324
Adiab Δ*E*, au		0.076 420	0.054 423	0.074 108	0.063 010
Adiab Δ*E*, cm^{-1}		16 772	11 945	16 265	13 829
			CI_2		
Gnd St *E*, au	−28.123 938	−27.818 858	−28.156 122	−27.892 794	−28.169 941
Exc St *E*, au	−28.070 791	−27.755 973	−28.113 927	−27.828 832	−28.117 424
Adiab Δ*E*, au	0.053 147	0.062 885	0.042 195	0.063 963	0.052 517
Adiab Δ*E*, cm^{-1}	11 657	13 802	9 261	14 038	11 526

[a] The transitions correspond to $^1B_1 \leftarrow {}^1A_1$ excitations for molecules with C_{2v} symmetry and $^1A'' \leftarrow {}^1A'$ excitations for molecules with C_s symmetry. [b] For HCBr and HCI, the higher level calculations were performed using 12 electrons in 9 active orbitals. [c] DNC = Did not converge.

in Table 5. These values range from a low of 9125 cm^{-1} to a high of 21 369 cm^{-1}. The trends in Table 5 correlate with the expectation that the largest transition energies correspond to the fluorine-containing species and the smallest to the iodine-containing species.

The adiabatic transition energies computed using the CASPT2 method are lower than those computed using the CASSCF method. For calculations involving two electrons in two active orbitals, the CASPT2 transition energies are 4400−4800 cm^{-1} lower than the CASSCF values. For calculations with 18 electrons in 12 active orbitals (or 12 electrons in 9 active orbitals for the HCX carbenes), the CASPT2 transition energies are 2200−3800 cm^{-1} lower than those obtained from the CASSCF calculations. These trends suggest that dynamic electron correlation effects included in the CASPT2 calculations are more important for the excited electronic states than the ground electronic states of these singlet halocarbenes. The excited-state energy is lowered to a greater extent than the ground-state energy, thus decreasing the energy gap between the two states.

The effects of increasing the active space on the adiabatic transition energies are variable. At the CASSCF level, the transition energies determined using the (18,12) active space for XCY carbenes or the (12,9) active space for HCX carbenes are generally lower by less than 800 cm^{-1} than the transition energies determined using the (2,2) active space. The exceptions are HCI, which shows an increase in transition energy of 1100 cm^{-1}, and CI_2, which shows an increase of 240 cm^{-1}. On the other hand, at the CASPT2 level, all of the transition energies are larger using the (18,12) or (12,9) active space than those determined using the (2,2) active space. The CASPT2(18,12) and CASPT2(12,9) results range from 1030 to 2270 cm^{-1} higher than the CASPT2(2,2) results. In this case, the increased active space lowers the ground-state energy more dramatically, leading to an increased spacing between the states.

Finally, where comparisons are available, the CASPT2-(18,12) or CASPT2(12,9) adiabatic transition energies are within 1000 cm^{-1} of the CISD results. In all cases, the CASPT2 values are lower than the CISD values.

While the SBKJC ECP basis set consistently overestimated the carbon−halogen bond lengths compared to experiment, adiabatic transition energies are very well predicted and are shown in Table 4 along with experimental values for HCBr, FCBr, and CBr_2. In their laser frequency modulation study, Sears and co-workers found a T_{oo} of 11 972.43 cm^{-1} for HCBr. This is in excellent agreement with the CASPT2(18,12) T_e value of 11 712 cm^{-1} and the CISD T_e value of 12 643 cm^{-1} from Table 4. Note that adding zero-point energy corrections to the values in Table 4 would in most cases bring the CASPT2(18,12) value even closer to experiment. As would be expected, the lower levels of theory are less accurate in predicting the adiabatic transition energies. For example, transition energies for HCBr computed at the CASSCF(2,2) and CASSCF(18,12) levels of theory differ by more than 2500 cm^{-1} from experiment. The CASPT2(2,2) T_e value, on the other hand, is only about 1300 cm^{-1} lower than the experimental value. It is clear from these comparisons that the dynamic electron correlation effects included in the CASPT2 method are essential for accurate determination of the adiabatic transition energies.

As can be seen in Table 4, there are both experimental and theoretical information about transition energies available for FCBr. Bacskay, Kable, and co-workers[30] calculated a T_{oo} value of 18 190 cm^{-1} at the CASPT2(18,12) level using the cc-pVTZ basis set. This result is some 2700 cm^{-1} below their own experimental value of 20 190 cm^{-1}. At the same level of theory, the SBKJC basis set used in the present study gave a T_e value of 21 369 cm^{-1}, only 1179 cm^{-1} from the experimental value. No other comparisons are available for FCBr because none of the other levels of theory were able to locate an optimized structure for the excited state.

The halocarbene from this work that has been the subject of numerous previous experimental and theoretical studies is CBr_2. Experimentally, Zhou et al.[18] and Xu and Harmony[15] used LIF to measure T_{oo} values of 14 885 and 15 092.7 cm^{-1}, respectively. Theoretically, Bacskay, Kable, and co-workers[27] calculated a T_e of 16 479 cm^{-1} at the CASSCF(18,12) level and a value of 14 114 cm^{-1} at the CASPT2(18,12) level with the cc-pVTZ basis set. These results differ from Xu and Harmony's supersonic free-jet expansion value by 1000 cm^{-1} or more. In the present study, the T_e value computed using the CISD level was 251 cm^{-1} higher than Xu and Harmony's experimental result, while the CASPT2(18,12) T_e value was only 99 cm^{-1} higher than experiment. The T_e values for CBr_2 and CFBr in the present study are consistently higher than those of Bacskay, Kable, and co-workers at the same level of theory. For example, the T_e value for CBr_2 at the CASPT2(18,12) level is 1078 cm^{-1} higher in the present work than the value computed by Bacskay, Kable, and co-workers. This difference can be attributed primarily to differences in the basis sets used. For example, adding one set of f-type polarization functions to the basis set used in this work leads to a decrease in T_e of 950 cm^{-1} for CBr_2.

IV. Conclusions

A series of bromine- and iodine-containing singlet carbenes was studied at the CASSCF, CASPT2, and CISD levels of theory. Through the use of the SBKJC effective core potential double-ζ basis set augmented with polarization functions, the structures and energies of the ground and first excited singlet states were determined. Overall, comparison of the results with previous studies utilizing all-electron basis sets (where available) indicates that the ECP basis set utilized in this work provides an excellent representation of both the ground and excited singlet states of bromo- and iodocarbenes. While the carbon−halogen bond lengths from these calculations were, in general, somewhat too long, adiabatic transition energies were in excellent agreement with experiment where comparisons were available. The transition energies for XCY (X, Y = F, Cl, Br, I) carbenes at the CASPT2(18,12) and CISD levels ranged from 11 500 to 21 400 cm^{-1}, leading to transition wavelengths primarily in the visible region, from 470 to 870 nm, with the exception being the transition wavelength for CI_2 at 870 nm. The transition wavelengths for HCX (X=Br, I) carbenes at the CASPT2(18,-12) and CISD levels were larger, ranging from 790 to 920 nm. The predicted transition wavelengths will allow further experimental studies to be carried out on these carbenes using the technique of cavity ringdown laser absorption spectroscopy.

Acknowledgment is made to the Illinois State University Research Grant program for support of portions of this work. R.W.Q. acknowledges Dr. Willie Hunter for the use of a computer used to carry out some of the calculations. J.M.S. acknowledges the National Center for Supercomputing Applications for a grant of supercomputer time.

References and Notes

(1) Molina, M. J.; Molina, L. T.; Kolb, C. E. *Annu. Rev. Phys. Chem.* **1996**, *47*, 327.
(2) Brahms, D. L. S.; Dailey, W. P. *Chem. Rev.* **1996**, *96*, 1585−1632.
(3) Storer, J. W.; Houk, K. N. *J. Am. Chem. Soc.* **1993**, *115*, 10426−10427.
(4) Hu, C.-H. *Chem. Phys. Lett.* **1999**, *309*, 81−89.
(5) Cramer, C. J.; Truhlar, D. G.; Falvey, D. E. *J. Am. Chem. Soc.* **1997**, *119*, 12338−12342.
(6) Sherrill, C. D.; Leininger, M. L.; Huis, T. J. V.; Schaefer, H. F. *J. Chem. Phys.* **1997**, *108*, 1040−1049.
(7) Gobbi, A.; Frenking, G. *Bull. Chem. Soc. Jpn.* **1993**, *66*, 6.
(8) Russo, N.; Sicila, E.; Toscano, M. *J. Chem. Phys.* **1992**, *97*, 5031−5036.
(9) Bunker, P. R.; Jensen, P.; Kraemer, W. P.; Beardsworth, R. *J. Chem. Phys.* **1986**, *85*, 3724−3731.
(10) Schwartz, R. L.; Davico, G. E.; Ramond, T. M.; Lineberger, W. C. *J. Phys. Chem. A* **1999**, *103*, 8213−8221.
(11) Lee, E. P. F.; Dyke, J. M.; Wright, T. G. *Chem. Phys. Lett.* **2000**, *326*, 143−150.
(12) Hajgato, B.; Minh ThiNguyen, H.; Veszpremi, T.; Tho Nguyen, M. *Phys. Chem. Chem. Phys.* **2000**, *2*, 5041−5045.
(13) Schwartz, M.; Marshall, P. J. *J. Phys. Chem.* **1999**, *103*, 7900−7906.
(14) Cao, J.; Ihee, H.; Zewail, A. H. *Chem. Phys. Lett.* **1998**, *290*, 1−8.
(15) Xu, S.; Harmony, M. D. *J. Phys. Chem.* **1993**, *97*, 7465−7470.
(16) Karolczak, J.; Joo, D. L.; Clouthier, D. J. *J. Chem. Phys.* **1993**, *99*, 1447−1456.
(17) Karolczak, J.; Clouthier, D. J. *J. Chem. Phys.* **1991**, *94*, 1−10.
(18) Zhou, S. K.; Zhan, M. S.; Shi, J. L.; Wang, C. X. *Chem. Phys. Lett.* **1990**, *166*, 547−550.
(19) Mathews, C. W. *Can. J. Phys.* **1967**, *45*, 2355−2374.
(20) Merer, A. J.; Travis, D. N. *Can. J. Phys.* **1966**, *44*, 525−547.
(21) Merer, A. J.; Travis, D. N. *Can. J. Phys.* **1966**, *44*, 1541−1550.
(22) Simons, J. P.; Yarwood, A. J. *Nature* **1961**, *192*, 943−944.
(23) Venkateswarlu, P. *Phys. Rev.* **1950**, *77*, 676−680.
(24) Chang, B.-G.; Costen, M. L.; Marr, A. J.; Ritchie, G.; Hall, G. E.; Sears, T. J. *J. Mol. Spectrosc.* **2000**, *202*, 131−143.
(25) Tsai, T.-C.; Chen, C.-W.; Chang, B.-C. *J. Chem. Phys.* **2001**, *115*, 766−770.
(26) Cai, Z. L.; Zhang, X.-G.; Wang, X.-Y. *Chem. Phys. Lett.* **1993**, *210*, 481−487.
(27) Sendt, K.; Bacskay, G. B. *J. Chem. Phys.* **2000**, *112*, 2227−2238.
(28) Schmidt, T. W.; Bacskay, G. B.; Kable, S. H. *J. Chem. Phys.* **1999**, *110*, 11277−11285.
(29) Schmidt, T. W.; Bacskay, G. B.; Kable, S. H. *Chem. Phys. Lett.* **1998**, *292*.

(30) Knepp, P. T.; Scalley, C. K.; Bacskay, G. B.; Kable, S. H. *J. Chem. Phys.* **1998**, *109*, 2220−2232.

(31) Cameron, M. R.; Kable, S. H.; Bacskay, G. B. *J. Chem. Phys.* **1994**, *103*, 4476−4483.

(32) Li, Z.; Francisco, J. S. *J. Chem. Phys.* **1998**, *109*, 134−138.

(33) Stevens, W. J.; Basch, H.; Krauss, M. *J. Chem. Phys.* **1984**, *81*, 6026.

(34) Stevens, W. J.; Basch, H.; Krauss, M.; Jasien, P. *Can. J. Chem.* **1992**, *70*, 612.

(35) Cundari, T. R.; Stevens, W. J. *J. Chem. Phys.* **1993**, *98*, 5555.

(36) Granovsky, A. A. http://classic.chem.msu.su/gran/gamess/index.html (accessed July 2000).

(37) Schmidt, M. W.; Baldridge, K. K.; Boatz, J. A.; Elbert, S. T.; Gordon, M. S.; Jensen, J. H.; Koseki, S.; Matsunaga, N.; Nguyen, K. A.; Su, S.; Windus, T. L.; Dupuis, M.; Montgomery, J. A. *J. Comput. Chem.* **1993**, *14*, 1347−1363.

(38) MOLPRO is a package of ab initio programs written by Werner, H.-J.; Knowles, P. J. with contributions from Amos, R. D.; Bernhardsson, A.; Berning, A.; Celani, P.; Cooper, D. L.; Deegan, M. J. O.; Dobbyn, A. J.; Eckert, F.; Hampel, C.; Hetzer, G.; Korona, T.; Lindh, R.; Lloyd, A. W.; McNicholas, S. J.; Manby, F. R.; Meyer, W.; Mura, M. E.; Nicklass, A.; Palmieri, P.; Pitzer, R.; Rauhut, G.; Schütz, M.; Stoll, H.; Stone, A. J.; Tarroni, R.; Thorsteinsson, T.

(39) Okabe, H. *Photochemistry of Small Molecules*; John Wiley & Sons: New York, 1978.

(40) Semekowitsch, J.; Zilch, A.; Carter, S.; Werner, H. J.; Rosmus, P. *Chem. Phys.* **1988**, *122*, 375.